

Heralded single photon absorption by a single atom

N. Piro, F. Rohde, C. Schuck, M. Almendros, J. Huwer, J. Ghosh, A. Haase, M. Hennrich, F. Dubin, and J. Eschner

ICFO - Institut de Ciències Fotoniques,
Mediterranean Technology Park, 08860 Castelldefels (Barcelona), Spain

*Corresponding author: juergen.eschner@icfo.es

Abstract. The emission and absorption of single photons by single atomic particles is a fundamental limit of matter-light interaction, manifesting its quantum mechanical nature. At the same time, as a controlled process it is a key enabling tool for quantum technologies, such as quantum optical information technology [1, 2] and quantum metrology [3, 4, 5, 6]. Controlling both emission and absorption will allow implementing quantum networking scenarios [1, 7, 8, 9], where photonic communication of quantum information is interfaced with its local processing in atoms. In studies of single-photon emission, recent progress includes control of the shape, bandwidth, frequency, and polarization of single-photon sources [10, 11, 12, 13, 14, 15, 16, 17], and the demonstration of atom-photon entanglement [18, 19, 20]. Controlled *absorption* of a single photon by a single atom is much less investigated; proposals exist but only very preliminary steps have been taken experimentally such as detecting the attenuation and phase shift of a weak laser beam by a single atom [21, 22], and designing an optical system that covers a large fraction of the full solid angle [23, 24, 25]. Here we report the interaction of single heralded photons with a single trapped atom. We find strong correlations of the detection of a heralding photon with a change in the quantum state of the atom marking absorption of the quantum-correlated heralded photon. In coupling a single absorber with a quantum light source, our experiment demonstrates previously unexplored matter-light interaction, while opening up new avenues towards photon-atom entanglement conversion in quantum technology.

Single trapped atomic ions provide optimal conditions for quantum information processing, meeting the requirements of high-fidelity state manipulation and detection schemes, as well as controlled interaction of the quantum bits [26, 27, 28]. At the same time, single photons are ideal carriers for transmitting quantum states and distributing entanglement over long distances [29]. Establishing quantum correlations between single atoms and single photons allows one to perform non-local atomic quantum gates mediated by photonic degrees of freedom, a key ingredient in quantum networks; this was demonstrated recently in experiments which created and employed entanglement between two remotely trapped ions [30, 31, 32]. These operations are based on the underlying entanglement between a single atom and its emitted photons. A fully bi-directional atom-photon interface implies transfer of quantum correlations also in the absorption of a photon; then entanglement can be distributed in a network by making two distant atoms interact with an entangled photon pair [33, 34]. Here, we report a step towards such entanglement transfer by observing the interaction between a single trapped ion and resonant, heralded single photons generated by spontaneous parametric down conversion (SPDC). We show that the time correlation shared by SPDC photon pairs is preserved in the interaction process, i.e. that absorption of a single photon by the ion is marked by the coincident detection of the second photon from the pair. More generally we demonstrate that dynamics of hybrid quantum systems involving atoms and quantum light can be controlled at the most fundamental limit of individual quantum particles.

Figure 1 displays schematically our experimental set-up. It combines a single trapped atomic ion with a continuous-wave source of entangled photon pairs. The $^{40}\text{Ca}^+$ ion is confined and laser-cooled in a linear Paul trap which is placed between two high numerical aperture laser objectives (HALOs) [35] collecting the ion's laser-excited fluorescence. The photon source emits coincident, frequency-correlated photon pairs with orthogonal polarizations in a 200 GHz spectral band centered at the frequency of the $D_{5/2}-P_{3/2}$ electronic transition of $^{40}\text{Ca}^+$, at 854 nm wavelength. For our experiments, the source is designed to interact resonantly with the $^{40}\text{Ca}^+$ ion [36, 37, 38]: the photon pairs are split, and on one of them we impose a frequency filtering to select "trigger" photons that match in frequency and bandwidth (25 MHz) the $D_{5/2}-P_{3/2}$ transition. The second, unfiltered photon is coupled to the ion through an optical fiber and one of the HALOs. As the two coincident photons are frequency-correlated [36], absorption events shall be accompanied by the simultaneous detection of a trigger photon that has passed the filter. The degree of such correlation between the detection of trigger photons and the recording of absorption events is controlled by the detuning of the filtering cavities with respect to the atomic resonance, and by the polarization of the photons exciting the ion.

Figure 2a presents the excitation sequence used to control the photon-ion interaction. Each period starts by a time interval during which the motion of the ion is laser-cooled. Excitation parameters of this part, i.e. intensities and detunings of the lasers and duration of the pulse, are optimized experimentally to ensure that the

ion is well localized and Doppler effects are negligible. Thereafter, the internal state of the ion is prepared using an optical pumping pulse: circularly polarized laser light at 854 nm, propagating along the quantization axis and resonant with the $D_{5/2}$ – $P_{3/2}$ electronic transition, pumps the ion into one of the two outer Zeeman sub-levels of the $D_{5/2}$ manifold, where it remains without scattering further photons. The appropriate helicity of the pump beam allows us to prepare an incoherent superposition of the states either with magnetic moments $m = \left\{\frac{3}{2}, \frac{5}{2}\right\}$, or with $m = \left\{-\frac{3}{2}, -\frac{5}{2}\right\}$. Finally, in the detection phase of the sequence, the ion is exposed to the unfiltered SPDC photons, whose polarization is controlled, while photodetectors are activated (PMT and APD in Fig. 1).

Absorption events during the detection phase are signaled by the onset of fluorescence, following the transfer of the electronic population from the $D_{5/2}$ to the $P_{3/2}$ manifold from which spontaneous decay occurs mainly towards the $S_{1/2}$ level (with 96% probability); this then leads to steady blue fluorescence induced by the laser excitation at 397 nm and 866 nm and recorded by the PMT photodetector. Meanwhile, the filtered trigger photons are detected on the APD photodetector. Figure 2b presents the signal of the two photodetectors to illustrate this process. For sufficiently high time resolution, as shown in Fig. 2c, we note that the arrival time of the first blue photon on the PMT coincides with the detection of a trigger photon on the APD. Hence, the time correlation initially shared by the photon pair has been transferred to the ion-photon system in this particular absorption event. To confirm this coincidence statistically, we compute the second-order time correlation function, $g^{(2)}(\tau)$, between detection events on the two detectors. Figure 2d shows that it exhibits a large peak at zero time delay showing that absorption of a single SPDC photon by the ion is marked by the coincident detection of a trigger photon. In the data presented in Fig. 2.d we observed a total of 1940 absorption events, at an average rate of 1.1 s^{-1} . These led to 175 coincidences, 20 being accidental, such that we deduce an overall 8% probability for the transfer of the temporal quantum correlation from photon pairs to ion and photon. While the absorption rate is determined by the brightness of the SPDC photon source [38], the transfer efficiency is set by the efficiency of coupling into the single-mode fiber used to excite the single ion ($\sim 60\%$), by the quantum efficiency of the APD detecting the filtered photons ($\sim 35\%$), and by the transmission through the filtering cavities ($\sim 45\%$).

With the ion optically pumped into the outer Zeeman sub-levels before the interaction, the rate of coincidences between absorption events and trigger photons is controlled by the polarization of the SPDC photons exciting the ion. We varied the polarization of the photons from right-circular to left-circular, thereby selecting excitation of transitions between $D_{5/2}$ and $P_{3/2}$ which involve a change of the magnetic moment by $\Delta m = -1$ or $+1$, respectively. Transitions with $\Delta m = 0$ are suppressed by exciting along the quantization axis. Fig. 3 shows the observed dependence for preparation of the ion in one of the two possible initial states, $m = \left\{\frac{3}{2}, \frac{5}{2}\right\}$, from which $\Delta m = 1$ transitions are not possible. The expected sinusoidal variation is found with $90 \pm 1\%$ visibility. Such polarization-selective absorption of a single photon is the key

to transferring the polarization degree of freedom from the photon to the ion, and is therefore the first step towards mapping photonic quantum information, including photonic entanglement, onto atomic qubits.

We also studied the influence of varying the transmission frequency of the filtering cavities. It should be noted that in this measurement the ion interacts always with the same broadband SPDC photons. Nevertheless, the frequency correlation between the trigger photon detected on the APD and its partner photon which may be absorbed by the ion makes the coincidence probability of these events depend on the filter frequency setting. This is shown in Figure 4 where we display the coincidence counts, $g^{(2)}(\tau = 0)$, as a function of the center frequency of the cavity filters. The two data sets correspond to the two different initial states of the ion, after optical pumping with σ^+ or σ^- light (see Fig. 2a). Coincidences are observed within the range of frequencies expected from the convolution of filter and transition bandwidth. The two spectra are displaced to higher and lower energies compared to the bare resonance of the $D_{5/2}-P_{3/2}$ transition. This is a consequence of the energy shift that the magnetic sub-states of the $D_{5/2}-P_{3/2}$ manifold experience in the applied magnetic field. The measured splitting of 9(2) MHz between the centers of the two spectra agrees, within the error, with the value of 12 MHz expected for the applied magnetic field of 5 Gauss. Like the polarization dependence, the control of the coincidence rate through the frequency of the trigger photons is another manifestation of the transfer of photon properties to the atom required in bidirectional photon-atom interfaces.

Acknowledgements. We acknowledge support by the European Commission (SCALA, Contract No. 015714; EMALI, MRTN-CT-2006-035369), the Spanish MICINN (QOIT, CSD2006-00019; QLIQS, FIS2005-08257; QNLP, FIS2007-66944; CMMC, FIS2007-29999-E), and the Generalitat de Catalunya [2005SGR00189; FI-AGAUR (C.S.)].

- [1] J. I. Cirac, P. Zoller, H. J. Kimble, and H. Mabuchi. Quantum state transfer and entanglement distribution among distant nodes in a quantum network. *Phys. Rev. Lett.*, 78(16):3221, 1997.
- [2] C. Monroe. Quantum information processing with atoms and photons. *Nature*, 416:238–246, 2002.
- [3] V. Giovannetti, S. Lloyd, and L. Maccone. Quantum-enhanced measurements: Beating the standard quantum limit. *Science*, 306(5700):1330–1336, NOV 19 2004.
- [4] D. Leibfried, M. D. Barrett, T. Schaetz, J. Britton, J. Chiaverini, W. M. Itano, J. D. Jost, C. Langer, and D. J. Wineland. Toward Heisenberg-limited spectroscopy with multiparticle entangled states. *Science*, 304(5676):1476–1478, JUN 4 2004.
- [5] P. O. Schmidt, T. Rosenband, C. Langer, W. M. Itano, J. C. Bergquist, and D. J. Wineland. Spectroscopy Using Quantum Logic. *Science*, 309(5735):749–752, 2005.
- [6] C. F. Roos, M. Chwalla, K. Kim, M. Riebe, and R. Blatt. 'designer atoms' for quantum metrology. *Nature* , 443:316–319, 2006.
- [7] H. J. Kimble. The quantum internet. *Nature*, 453:1023–1030, 2008.
- [8] L. Luo, D. Hayes, T. A. Manning, D. N. Matsukevich, P. Maunz, S. Olmschenk, J. D. Sterk, and C. Monroe. Protocols and techniques for a scalable atom-photon quantum network. *Fortschr. d. Phys.*, 57:1133–1152, 2009.
- [9] L. Duan and C. Monroe. Quantum networks with trapped ions. *Rev. Mod. Phys.*, to appear; preprint <http://www.iontrap.umd.edu/publications/archive/DuanMonroeReview2009.pdf>, 2010.
- [10] M. Keller, B. Lange, K. Hayasaka, W. Lange, and H. Walther. Continuous generation of single photons with controlled waveform in an ion-trap cavity system. *Nature*, 431:1075, 2004.
- [11] T. Wilk, S. C. Webster, H. P. Specht, G. Rempe, and A. Kuhn. Polarization-controlled single photons. *Physical Review Letters*, 98(6):063601, 2007.
- [12] T. Legero, T. Wilk, M. Hennrich, G. Rempe, and A. Kuhn. Quantum beat of two single photons. *Phys. Rev. Lett.*, 93(7):070503, 2004.
- [13] M. Hijlkema, B. Weber, H. P. Specht, S. C. Webster, A. Kuhn, and G. Rempe. A single-photon server with just one atom. *Nature Physics*, 3:253–255, 2007.
- [14] J. McKeever, A. Boca, A. D. Boozer, R. Miller, J. R. Buck, A. Kuzmich, and H. J. Kimble. Deterministic Generation of Single Photons from One Atom Trapped in a Cavity. *Science*, 303(5666):1992–1994, 2004.
- [15] P. Maunz, D. L. Moehring, S. Olmschenk, K. C. Younge, D. N. Matsukevich, and C. Monroe. Quantum interference of photon pairs from two remote trapped atomic ions. *Nat. Phys.*, 3:538, 2007.
- [16] H. G. Barros, A. Stute, T. E. Northup, C. Russo, P. O. Schmidt, and R. Blatt. Deterministic single-photon source from a single ion. *New Journal of Physics*, 11(10):103004, 2009.
- [17] M. Almendros, J. Huwer, N. Piro, F. Rohde, C. Schuck, M. Hennrich, F. Dubin, and J. Eschner. Bandwidth-tunable single-photon source in an ion-trap quantum network. *Phys. Rev. Lett.*, 103(21):213601, 2009.
- [18] B. B. Blinov, D. L. Moehring, L. M. Duan, and C. Monroe. Observation of entanglement between a single trapped atom and a single photon. *Nature*, 428:153, 2004.
- [19] J. Volz, M. Weber, D. Schlenk, W. Rosenfeld, J. Vrana, K. Saucke, C. Kurtsiefer, and H. Weinfurter. Observation of entanglement of a single photon with a trapped atom. *Phys. Rev. Lett.*, 96(3):030404, 2006.
- [20] T. Wilk, S. C. Webster, A. Kuhn, and G. Rempe. Single-atom single-photon quantum interface. *Science*, 317(5837):488–490, 2007.
- [21] M. K. Tey, Z. Chen, S. A. Aljunid, B. Chng, F. Huber, G. Maslennikov, and C. Kurtsiefer. Strong interaction between light and a single trapped atom without the need for a cavity. *Nat Phys*, 4(12):924–927, December 2008.
- [22] S. A. Aljunid, M. K. Tey, B. Chng, T. Liew, G. Maslennikov, V. Scarani, and C. Kurtsiefer. Phase shift of a weak coherent beam induced by a single atom. *Phys. Rev. Lett.*, 103(15):153601, Oct 2009.

- [23] M. Sondermann, R. Maiwald, H. Konermann, N. Lindlein, U. Peschel, and G. Leuchs. Design of a mode converter for efficient light-atom coupling in free space. *Applied Physics B: Lasers and Optics*, 89(4):489–492, December 2007.
- [24] R. Maiwald, D. Leibfried, J. Britton, J. C. Bergquist, Leuchs G., and Wineland D. J. Stylus ion trap for enhanced access and sensing. *Nature Physics*, 5:551–554, 2009.
- [25] G. Wrigge, I. Gerhardt, J. Hwang, G. Zumofen, and V. Sandoghdar. Efficient coupling of photons to a single molecule and the observation of its resonance fluorescence. *Nature Physics*, 4:60–66, 2008.
- [26] D. Leibfried, R. Blatt, C. Monroe, and D. Wineland. Quantum dynamics of single trapped ions. *Rev. Mod. Phys.*, 75:281, 2003.
- [27] H. Haefner, C. F. Roos, and R. Blatt. Quantum computing with trapped ions. *Phys. Rep.*, 469:155, 2008.
- [28] R. Blatt and D. Wineland. Entangled states of trapped atomic ions. *Nature*, 443:1008–1014, 2008.
- [29] R. Ursin, F. Tiefenbacher, T. Schmitt-Manderbach, H. Weier, T. Scheidl, M. Lindenthal, B. Blauensteiner, T. Jennewein, J. Perdigues, and et al. P. Trojek. Entanglement-based quantum communication over 144 km. *Nat. Phys.*, 3:481–486, 2007.
- [30] D. L. Moehring, P. Maunz, S. Olmschenk, K. C. Younge, D. N. Matsukevich, L.-M. Duan, and C. Monroe. Entanglement of single-atom quantum bits at a distance. *Nature*, 449(7158):68–71, sep 2007.
- [31] P. Maunz, S. Olmschenk, D. Hayes, D. N. Matsukevich, L.-M. Duan, and C. Monroe. Heralded quantum gate between remote quantum memories. *Phys. Rev. Lett.*, 102(25):250502, Jun 2009.
- [32] S. Olmschenk, D. N. Matsukevich, P. Maunz, D. Hayes, L.-M. Duan, and C. Monroe. Quantum teleportation between distant matter qubits. *Science*, 323(5913):486–489, 2009.
- [33] S. Lloyd, M. S. Shahriar, J. H. Shapiro, and P. R. Hemmer. Long distance, unconditional teleportation of atomic states via complete bell state measurements. *Phys. Rev. Lett.*, 87(16):167903, Sep 2001.
- [34] B. Kraus and J. I. Cirac. Discrete entanglement distribution with squeezed light. *Phys. Rev. Lett.*, 92(1):013602, Jan 2004.
- [35] S. Gerber, D. Rotter, M. Hennrich, R. Blatt, F. Rohde, C. Schuck, M. Almendros, R. Gehr, F. Dubin, and J. Eschner. Quantum interference from remotely trapped ions. *New Journal of Physics*, 11(1):013032, 2009.
- [36] A. Haase, N. Piro, J. Eschner, and M. W. Mitchell. Tunable narrowband entangled photon pair source for resonant single-photon single-atom interaction. *Opt. Lett.*, 34(1):55–57, January 2009.
- [37] N. Piro, A. Haase, M. W. Mitchell, and J. Eschner. An entangled photon source for resonant single-photon single-atom interaction. *Journal of Physics B: Atomic, Molecular and Optical Physics*, 42(11):114002–, 2009.
- [38] C. Schuck, F. Rohde, N. Piro, M. Almendros, J. Huwer, M. W. Mitchell, M. Hennrich, A. Haase, F. Dubin, and J. Eschner. Resonant interaction of a single atom with single photons from a down-conversion source. *Phys. Rev. A*, 81(1):011802, Jan 2010.

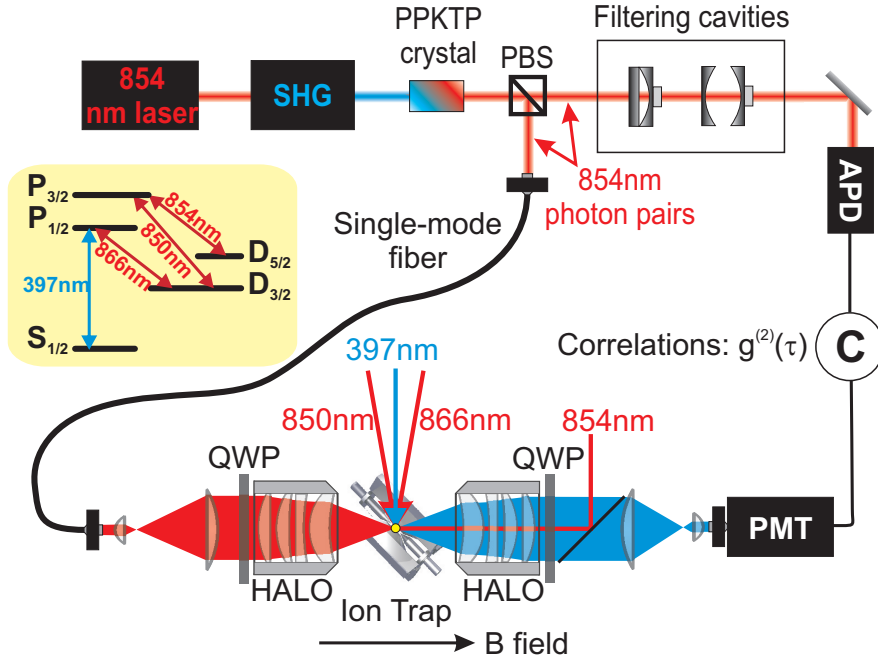


Figure 1. Experimental setup. A single $^{40}\text{Ca}^+$ ion is confined in a radio-frequency ion trap placed between two high-numerical-aperture lenses (HALOs). The ion is laser-cooled by laser light at 397 nm and 866 nm, entering the trap from the side. Lasers at 850 nm and 854 nm are used for state preparation; relevant atomic levels and transitions are schematically represented in the inset. A magnetic field provides a quantization axis along the optical axis of the HALOs. Each HALO collects about 4% of the 397 nm fluorescence photons, which are thereafter detected by a photomultiplier tube (PMT). One HALO is also utilized to focus photons from the pair source onto the ion. The photon pair source is based on a narrowband, frequency-stabilized diode laser (master laser) tuned to the $D_{5/2}-P_{3/2}$ transition in $^{40}\text{Ca}^+$ at 854 nm. After frequency doubling (second harmonic generation, SHG), the 427 nm light is focused into a periodically poled KTP (PPKTP) nonlinear crystal designed to produce photon pairs around 854 nm by spontaneous parametric down-conversion (SPDC). The crystal is operated in type-II collinear phase-matching configuration, such that pairs of orthogonally polarized photons are generated in a single spatial mode. A polarizing beam splitter (PBS) spatially splits the photon pairs. One output mode is coupled through a single-mode fiber and focussed onto the single ion through one HALO. In the second output we employ a spectral filtering stage, consisting of two cascaded Fabry-Perot cavities, whose transmission frequency is actively stabilized to the 854 nm master laser, while their transmission bandwidth of 22 MHz is tailored to match the one of the 854 nm atomic transition [36, 37]. Photons transmitted through the filter are sent to an avalanche photodiode (APD), and detection events are correlated with the arrival times of blue fluorescence photons at the PMT. Quarterwave plates (QWP) allow controlling the polarization of the SPDC photons and of the 854 nm laser light.

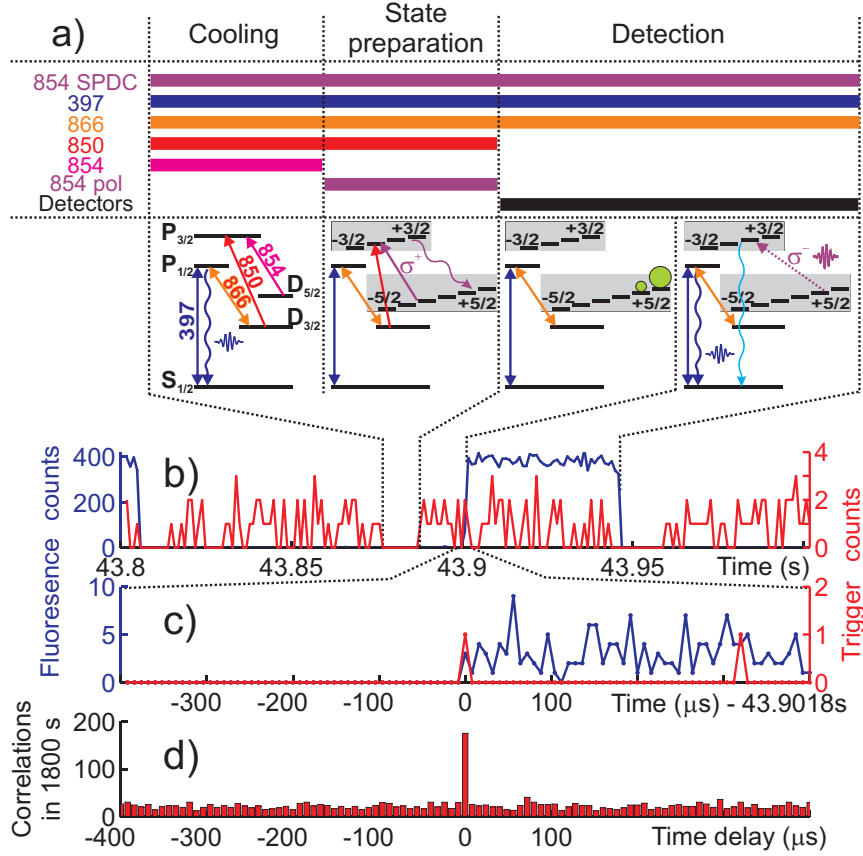


Figure 2. Interaction process. a) Periodic laser pulse sequence used to control and observe the ion-photon interaction. It first consists of a cooling phase lasting 5 ms followed by state preparation and detection phases of 5 and 60 ms respectively. At the end of the preparation phase, the internal state of the ion is deterministically initialized in sub-levels of the $D_{5/2}$ manifold with magnetic quantum numbers $m = \{\frac{3}{2}, \frac{5}{2}\}$ (or $\{-\frac{3}{2}, -\frac{5}{2}\}$, not shown), which couple to the excited $P_{3/2}$ state through σ^- (σ^+) transitions; thereby the possible absorption of a photon in the detection phase is controlled. An absorption event results in the onset of emission of 397 nm fluorescence by the ion. This is illustrated in (b), where a time trace of fluorescence counts on the PMT is displayed with 1 ms time resolution (blue line); detected trigger photons transmitted through the filtering cavities are also shown (red). Increasing the time resolution to 8 μ s (c), we note that the photon absorption event, marked by the first detected 397 nm photon, is coincident with the detection of its trigger photon. The correlation between the two events is statistically verified by a strong peak at zero time delay in the corresponding $g^{(2)}(\tau)$ -correlation function, displayed in (d) for a total recording time of 30 min.

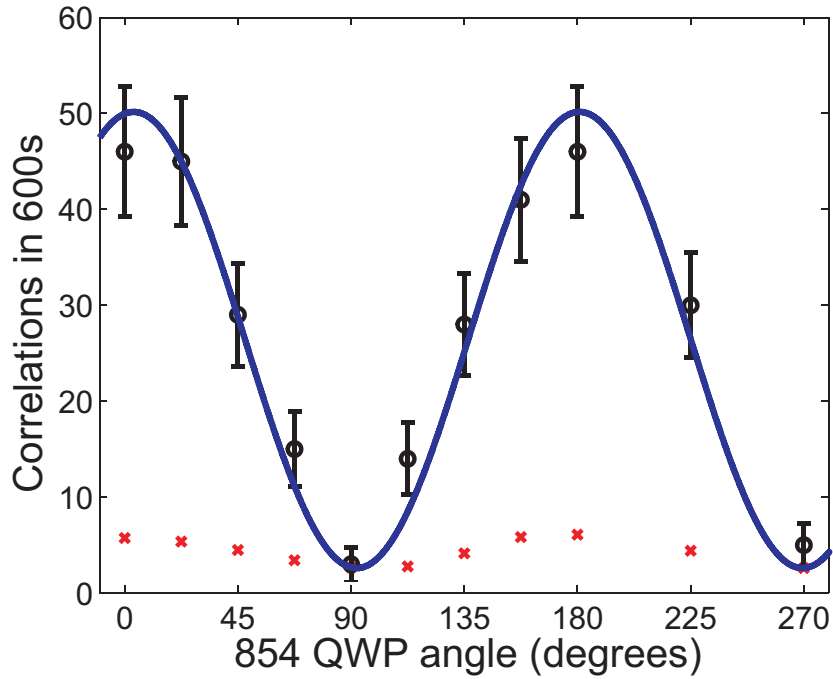


Figure 3. Dependence on photon polarization. The ion is prepared in an incoherent superposition of magnetic sub-levels $m = \{\frac{3}{2}, \frac{5}{2}\}$ of the $D_{5/2}$ manifold before exposure to the SPDC photons. For various settings of the photon polarization (QWP angle), the number of coincidences between absorption events and heralding photons is measured during 10 min, corresponding to the value of the $g^{(2)}$ correlation function at $\tau = 0$ (circles). The coincidence rate reaches a maximum value of $\approx 5\text{min}^{-1}$ for σ^- polarized photons (QWP angle of 0°) and reduces to the background level (red crosses) for σ^+ polarized photons (90°). Displayed error bars correspond to one standard deviation assuming Poissonian counting statistics. A visibility of $90 \pm 1\%$, without subtracting accidental coincidences, is derived from a least-squares sinusoidal fit (solid curve).

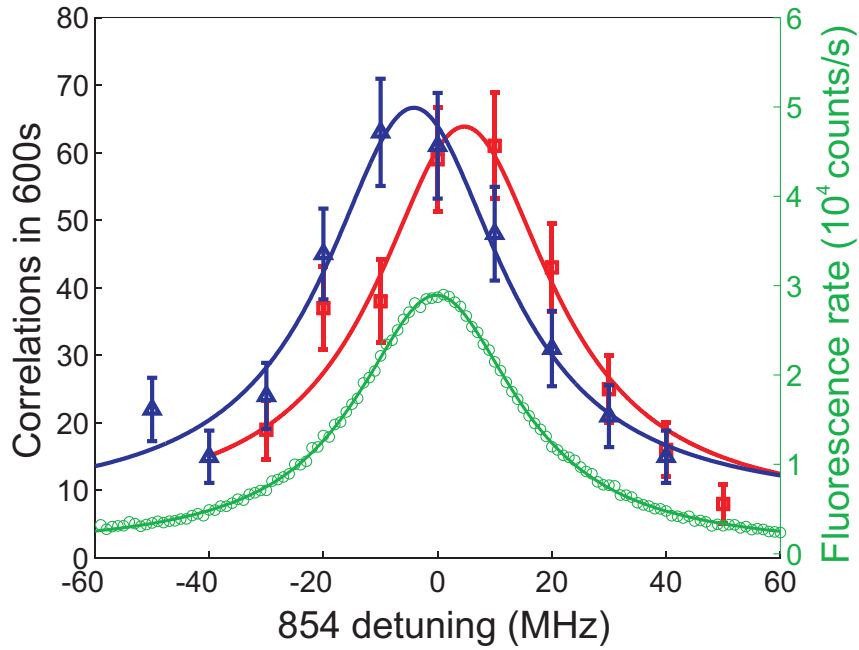


Figure 4. Correlation spectroscopy with single photons. The rate of coincidences between absorption events and trigger photon detection is varied by controlling the central frequency of the filter cavities. Red squares (blue triangles) show data taken with the 854 nm pumping laser σ^+ (σ^-) polarized and the SPDC photons set to σ^- (σ^+). Each data point corresponds to the value of $g^{(2)}(\tau = 0)$ obtained after 10 minutes of acquisition. Poissonian error bars are also displayed. The center frequency of the $D_{5/2}$ - $P_{3/2}$ transition is set to 0 MHz and deduced from fluorescence spectroscopy with a vertically polarized 854 nm laser and without optical pumping (green circles). Solid lines show least-squares Lorentzian fits to the data points.